

Luminescent Terbium Doped Aluminate Particles: Properties and Surface Modification with Asparagine

José M. A. Caiut,^{*,a,b,c} Younes Messaddeq,^a Hervé Dexpert,^b Marc Verelst,^b
Sidney J. L. Ribeiro^a and Jeannette Dexpert-Ghys^b

^aInstituto de Química, Universidade Estadual Paulista - UNESP,
CP 355, 14801-970 Araraquara-SP, Brazil

^bCentre for Materials Elaboration and Structural Studies/CNRS, BP 4347,
31055 Toulouse CEDEX 4, France

^cDepartamento de Química, Faculdade de Filosofia, Ciências e Letras de Ribeirão Preto,
Universidade de São Paulo, 14040-901 Ribeirão Preto-SP, Brazil

New luminescent organic-inorganic hybrid particles based on Tb-doped aluminates and asparagine (Asn) surface modifiers were investigated. The Tb³⁺ doped inorganic core was obtained by spray pyrolysis, at 200 °C γ -AlOOH (BOE:Tbx%) or at 700 °C γ -Al₂O₃ (γ TA:Tbx%). The reaction of Asn with boehmite in water disaggregated the sub-micronic boehmite particles to give stable dispersion of surface modified nanoparticles Asn:BOE:Tbx% (x = 1 or 5). Concerning the Asn: γ TA:Tbx% system, an Asn film wrapping alumina particles was observed. Photoluminescence spectra exhibited the bands assigned to Tb³⁺ ⁵D₄ → ⁷F_{J=6,3} transitions. A broad absorption band (240 nm) was assigned to the host (aluminate) to ion (Tb³⁺) energy transfer. Efficient energy transfer was observed when active ions are incorporated in the defect-spinel structure of γ TA, whereas it was relatively weak for BOE:Tb where Tb³⁺ are bonded to the hydroxyls groups at nanocrystals surface. It is noticeable that Asn strengthens the linkage of Tb³⁺ with the aluminate matrix, enhancing the host to dopant energy transfer.

Keywords: hybrid, spray pyrolysis, alumina, rare earth, terbium luminescence

Introduction

“Alumina” is the general name encompassing a large number of products with different chemical formulas and/or structures. The thermodynamically stable phase at standard temperature and pressure conditions is α -Al₂O₃, having the hexagonal crystal structure of the mineral corundum. Lanthanide ions doped alumina (α) provide extremely versatile photoluminescent ceramics. The green emitter Tb³⁺ was for instance successfully incorporated into a dense alumina matrix, achieving a transparent light-emitting ceramic.¹ Transitions alumina's (partially dehydrated aluminum hydroxides) possess high surface areas which renders them appropriate for use as adsorbents, catalysts and catalyst carriers. The “ γ -Al₂O₃” transition alumina is particularly important in catalysis and details of its structure and exact composition have been the subject of a

number of controversial works.²⁻⁷ Boehmite, γ -AlOOH, is actually the most important precursor for the synthesis of transition aluminas following the transformation sequence boehmite → γ → δ → θ → α . Crystallization degree, morphology and surface properties are observed to be highly dependent on the structure.

Nanocrystalline boehmite can be obtained through a sol-gel route as firstly described by Yoldas.^{8,9} Nanocrystalline boehmite may be employed as sorbent, for instance by removing potentially toxic metal from polluted waste water.¹⁰ The surface of boehmite particles is highly reactive towards carboxylic acids in aqueous media. The adsorption of low molecular weight carboxylic acids, ubiquitous in natural environments, on positively charged mineral surfaces, e.g., aluminium oxihydroxides, has also been the subject of many investigations.¹¹

Material chemists have taken benefit of this high affinity to synthesize alumoxanes from the reaction of boehmite with carboxylic acids.¹² Once formed, the carboxylate-

*e-mail: caiut@ffclrp.usp.br

substituted alumoxanes may be employed as precursors for a wide range of ceramics, including lanthanide-aluminium mixed-metal oxides.¹³

Alumina-based nanoparticles or nano-structured objects with possible applications in the field of nano-bio-technology or nano-medicine have been described. Alumina membranes with highly ordered nanopores are proposed for instance in smart implantable drug delivery systems.¹⁴ Although far less described in literature than mesoporous silica, powdered mesoporous (hydrated) alumina is a potentially available substrate for controlled drug release, after suitable chemical functionalization of its surface.¹⁵

On the other hand, luminescent micro- or nanoparticles are becoming of great importance in the field of bio-labeling. Several examples of crystalline lanthanide oxides as luminescent biolabels are also found in literature. Eu^{3+} and Tb^{3+} containing nanomaterials have also been reported as in nanocrystalline hydroxyapatite or in lanthanum phosphate for example.¹⁶⁻¹⁸ Lanthanide emitters (Eu^{3+} , Tb^{3+}) are particularly interesting for the purpose of luminescent bio-labeling since the decay times for the main intra $4f^n$ transitions are much longer than the decay times of the background fluorescence of biological samples. By employing well-suited experimental set-ups the photoluminescence signal from the optical probe may be discriminated from the background emission from all non-probed species.¹⁹

Concerning preparation methods spray pyrolysis (SP) is an aerosol process commonly used to form a variety of materials in powder form, including transition aluminas or α alumina.²⁰⁻²² A protocol based on the rapid drying of an aluminium alcoholate suspension was proposed in order to synthesize nanocrystalline γ - AlOOH or γ - Al_2O_3 in a single step, by the SP process.²³ Moreover, by the addition of an optically active lanthanide ion Eu^{3+} or Tb^{3+} , luminescent aluminates can be obtained in just one step.²⁴⁻²⁶

Due to its high affinity for the boehmite surface, the amino-acid asparagines (Asn) strengthens the attachment of the luminescent europium ions at the boehmite nanoparticles after their suspension in water.²⁴

On the basis of these preceding observations, we present here a systematic investigation of Asn:aluminates:Tb nanostructured particles. Terbium-doped aluminates, having the boehmite (BOE) or the gamma alumina structure were obtained by spray pyrolysis, and will be noted BOE:Tbx% and γ TA:Tbx%, respectively. The luminescence properties of these powders will be discussed regarding the possible sites of terbium ions in the aluminates and the effects of matrix-dopant electronic interactions. The possibility of modifying the surface of these aluminates by the amino acid Asn was then explored.

Asparagine ($\text{Asn} = \text{H}_2\text{N}-\text{CO}-\text{CH}(\text{NH}_3^+)-\text{COO}^-$ at $\text{pH} = 7.0$) was chosen to render the oxide particles bio-compatible, because the carboxylic end will presumably attach the aluminate surface, with the formation of alumoxanes, whereas the amide group will be let free for further reaction. Hereafter, composites with Asn will be compared with the corresponding un-modified aluminate, to highlight the organic-inorganic interactions. Finally, the possibility to achieve luminescent nano-labels in the investigated systems will be discussed.

Experimental

Hydrated alumina samples were prepared by spray pyrolysis. The precursor (boehmite sol) was obtained by the methodology established by Yoldas modified to obtain the rare earth doped alumina.^{8,9} TbCl_3 (0.37 g, 0.001 mol) was dissolved in water (300 mL) at 80 °C. Aluminum tri-*sec*-butoxide (25.93 g, 0.1 mol) was added to terbium aqueous solution under stirring at 80 °C. After 2 h stirring, nitric acid was added as a peptizing agent, up to 0.07 $\text{HNO}_3/\text{Al}^{3+}$ (molar ratio). The sol (with concentration adjusted to 0.2 mol L^{-1} Al^{3+} by water dilution) was spray dried in an experimental setup already described.²³ In this setup, the spray was generated by a piezoelectric pellet oscillating at 2.4 MHz. The aerosol, made of fine droplets (ϕ ca. 5 μm) from the precursor solution in air, was then driven into two heating zones, the first one around 100 °C and the second one was the decomposition-densification zone where the temperature may be adjusted at a chosen temperature (T_{SYN}). The powder was separated from the gas phase by an electrostatic collector. The drying and decomposition were accomplished within about 10 s. T_{SYN} was fixed at 200 °C for the synthesis of boehmite (BOE), and at 700 °C for that of the “ γ ” transition alumina (γ TA). Three dopant percentages were investigated: 1, 5 and 10% expressed in mol of Tb^{3+} /mol of Al^{3+} .

Amino acids

Aluminoxanes nanocomposites were obtained by dispersing the hydrated aluminas particles in Asn water solutions. Samples activated with Tb1% (BOE:Tb1% or γ TA:Tb1%) were dispersed in water (300 mg in 25 mL). Asn was added (1/0.1, 1/0.3 or 1/0.5 mol Al/Asn) and kept under stirring at room temperature for 12 hours. The reaction mixture was centrifuged and the solid was rinsed three times with distilled water and ethanol. The particles were dried at 80 °C and characterized by X-ray diffraction, electron microscopy, Fourier transform infrared spectroscopy and luminescence. Water suspensions were

used for dynamic laser light scattering measurements and also to complete the analysis of Tb^{3+} luminescence. For the high Asn composition (0.5Asn:1BOE:Tb1%), the sample was observed to be composed off a mixture of nanoparticles and crystallized Asn; concerning the lower content (0.1 Asn), changes on alumina particles were not measureable. Therefore only results obtained for compositions 0.3Asn:1Al will be presented. Composite samples will be named Asn:BOE:Tb (% , mol Tb/Al) and Asn: γ TA:Tb (% , mol Tb/Al).

Characterization

The powders were characterized by X-ray diffraction (XRD), with a Seifert XRD3000 diffractometer. The coherent length was estimated with the Scherrer equation ($D = 0.91 (FWHM) \cos\theta$) with the full width at half maximum measured in (2θ) and expressed in radians. The size distributions of powders dispersed in water were determined by dynamic laser light scattering (DLS) using a Malvern Instruments ZETASIZER 3000, model DTS5300.

Samples were observed by transmission electron microscopy (TEM) with a Philips-CM120 and by scanning electron microscopy (SEM) with a SEM-JEOL 6700F. Fourier transform infrared (FTIR) spectra were recorded in KBr pellets using a model 2000 Perkin-Elmer spectrometer. Room temperature luminescence excitation and emission spectra were measured with a Hitachi-FI100 spectrofluorimeter (at 2.5 nm spectral resolution) for solids samples. The 5D_4 lifetime measurements were obtained by coupling a phosphorimeter to a spectrofluorimeter SPEX Fluorolog, model F212I, monitoring the emission intensity at 543 nm. Finally, a Varian ECLIPSE (model EI05123699) operating in time-resolved mode with excitation and emission band-passes of 10 nm was employed to record the spectra of particles in suspension.

Results and Discussion

XRD and FTIR: structural investigations

Investigations by X-ray diffraction (Figure 1) and FTIR spectroscopy (Figure 2) confirmed that powders synthesized at 200 and 700 °C were boehmite γ -AlOOH and γ -Al₂O₃, respectively, both being weakly crystallized and with a high degree of hydration. Surface modification by Asn induced tenuous changes as discussed hereafter.

At $T_{SYN} = 200$ °C the diffractogram matched with the reference JCPD No. 21-1307. In a former paper, details of X-ray data of boehmite samples elaborated by SP have been analyzed.²⁴ The average nanocrystal size following the

orthorhombic axis *b* does not exceed one cell, so that half the hydroxyl groups are at the external surface of nanocrystals. At $T_{SYN} = 700$ °C, the diffractogram corresponded to reference data JCPD No. 10-0425: with peaks labeled (400) and (440) at $2\theta = 46$ and 66.5° , respectively, and a very broad and asymmetrical band between 30 and 40° , which contains the badly resolved contributions from (220) and (311) planes. The peak positions matched with the gamma-alumina standard apart from the absence of (111) and (222), which should be observed in well crystallized transition aluminas.^{2,5} The coherent length evaluated was about 3 nm for the SP transition aluminas, but the important background observed under the peaks supports that the size of most nanocrystals in the samples were below this value. On reacting with asparagine, an additional broad band appeared at 2θ ca. 20° for boehmite samples, assigned to the organic counterpart of the composite. The reaction of γ -Al₂O₃ with Asn has lead to the partial transformation of γ -Al₂O₃ into γ -AlOOH, the diffraction peaks of γ -AlOOH being marked by stars in Figure 1B.

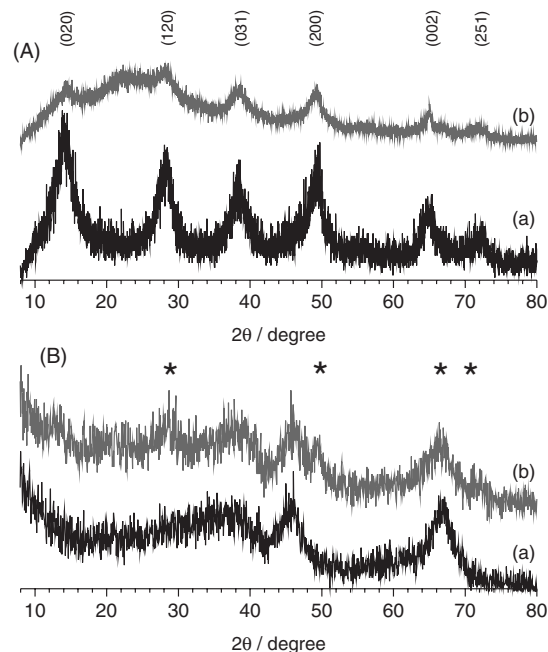


Figure 1. Powder X-ray diffraction (A) (a) BOE:Tb1% and (b) Asn:BOE:Tb1%. (B) (a) γ TA:Tb1% and (b) Asn: γ TA:Tb1%. (*) denote γ -AlOOH phase in γ -Al₂O₃.

FTIR spectrum of boehmite γ -AlOOH has been described in literature.^{27,28} In agreement with these previous papers, the spectrum recorded for the powder $T_{SYN} = 200$ °C (Figure 2A) displayed vibrational modes of [AlO₆] at 481, 632, 734 cm^{-1} and δ_{OH} at 1072 and 1157 cm^{-1} . Samples were highly hydrated, as were amorphous or nanocrystallized boehmite described in references.^{28,29} The two δ_{OH} modes at 3083 and 3310 cm^{-1} were partly obscured by the broad

band around 3400 cm^{-1} , this last one assigned to adsorbed hydroxyls. The presence of adsorbed water molecules was evidenced by the δ_{HOH} at 1630 cm^{-1} . FTIR spectrum of sample $T_{\text{SYN}} = 700\text{ }^{\circ}\text{C}$ (Figure 2B) was quite in agreement, in the wave number range $400\text{--}1400\text{ cm}^{-1}$, with the one of $\gamma\text{-Al}_2\text{O}_3$,²⁸ with relatively broad bands peaking at 635 cm^{-1} (stretching AlO_6) and 785 cm^{-1} (stretching AlO_4). Adsorbed water and hydroxyls were attested at 1630 cm^{-1} and around 3400 cm^{-1} .

Boehmite and aluminates from spray pyrolysis displayed features around 1385 cm^{-1} from residual nitrates but no trace of organics from the preparation mixture were detected. The band at 1673 cm^{-1} (C=O) and CH vibrations at 1360 , 1316 and 1236 cm^{-1} were well isolated for sample 0.3Asn:BOE:Tb1\% . Additional features were observed at 1500 cm^{-1} and superimposed with the hydroxyls modes in the region $3000\text{--}3400\text{ cm}^{-1}$, but were not assigned. In the spectrum of $\text{Asn:}\gamma\text{TA:Tb1\%}$, shown in Figure 2B, only very weak effect from the organic part was detectable, as a low intensity band at 1416 , 1428 and 1511 cm^{-1} δCN , $\nu_s\text{ CO}_2^-$ and $\delta\text{ NH}_3^+$ vibration, respectively.³⁰ Important changes were observed in the aluminate response since

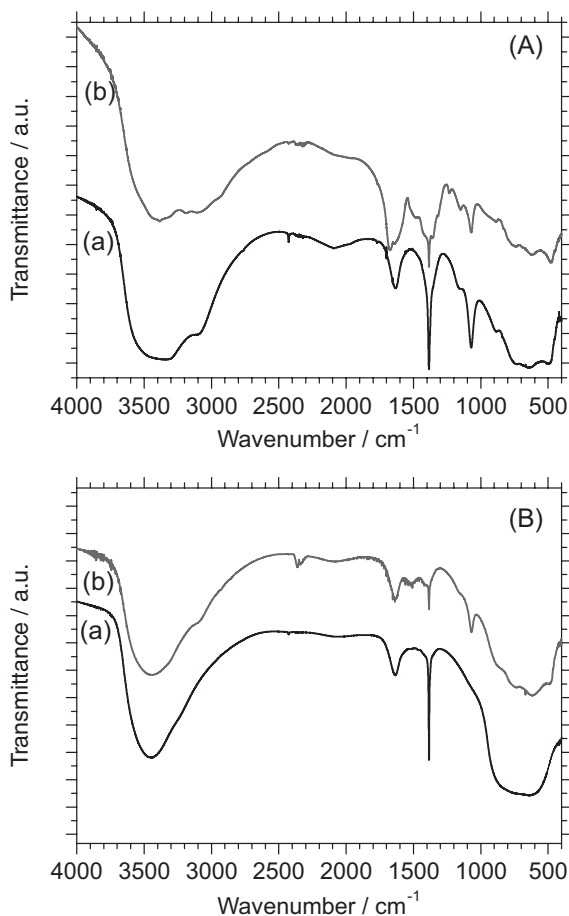


Figure 2. (A) FTIR spectra of (a) BOE:Tb1% and (b) Asn:BOE:Tb1%. (B) FTIR spectra of (a) $\gamma\text{TA:Tb1\%}$ and (b) Asn: $\gamma\text{TA:Tb1\%}$.

bands characteristic of boehmite were observed proving the partial transformation of $\gamma\text{-Al}_2\text{O}_3$ into $\gamma\text{-AlOOH}$, also evidenced by XRD.

Morphology and water dispersion

The particles prepared by spray pyrolysis were always spherical and sub-micrometric with a moderately dispersion in size, whatever their composition. The major fraction of hydrated alumina particles presents diameters between 100 and 500 nm . Some characteristic electron microscope images are gathered in Figure 3. SEM images recorded on BOE:Tb1%, Figure 3a, and on $\gamma\text{TA:Tb1\%}$, Figure 3b, evidence irregular surfaces, and spherical particles consisting of smaller (nanometric) sub-particles, aggregated in the spray pyrolysis processing. TEM observations, Figures 3c and 3d, give additional information since the spheres were homogeneously packed with sub-particles, and not hollow, although hollow particles can be obtained by SP.²²

In composite materials, the organic and inorganic counterparts could be well observed, the effect of the dispersant being more noticeable on boehmite than on transition alumina particles. Most of the boehmite spheres had disaggregated during reaction with Asn. Sample Asn:BOE:Tb1\% , shows an organic film in which the nanoparticles appear dispersed. TEM image Figure 3e shows the composite film and one bigger particle not completely disaggregated. Aluminum was identified by local analysis (EDXS in TEM) throughout the film. Figure 3f was recorded on the film in dark field conditions: all bright parts are due to crystallized boehmite nanoparticles (a few nm in size), embedded in the amorphous polymer. For sample $\text{Asn:}\gamma\text{TA:Tb1\%}$ (TEM image in Figure 3g), the organic film was observed to wrap the sub micrometric alumina particles.

Asn molecules were observed to interact differently with boehmite and Al_2O_3 . Boehmite^{23,24} micrometric spheres obtained by SP had been spontaneously dispersed in water. The same remark was made here for BOE:Tb1% by DLS analysis. 60% of the particles fall in the range $25\text{--}40\text{ nm}$, while higher values (up to 85 nm) were measured for the remaining 40%. Spherical sub-micrometric particles were disaggregated in water and nanometric sub-particles remained very stable. At 5 or 10% Tb^{3+} particles were noticeably bigger: higher contents in Ln^{3+} lead to more tightly linked sub-particles. Once formed, these spherical microparticles had not been fragmented in water. In addition, all particles synthesized at $T_{\text{SYN}} = 700\text{ }^{\circ}\text{C}$ with the $\gamma\text{-Al}_2\text{O}_3$ structure, remained stable in water. The addition of Asn did not change the particles form and the

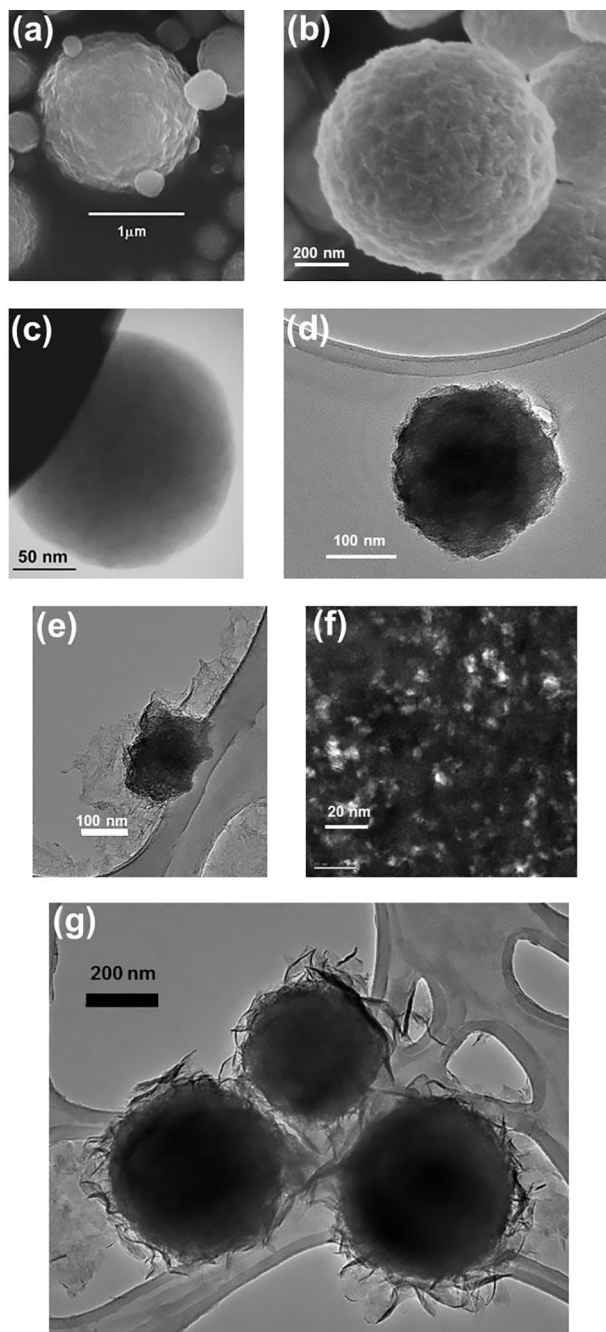


Figure 3. Electron microscopy images, SEM (a) BOE:Tb1%; (b) γ TA:Tb1%; TEM (c) BOE:Tb1%; (d) γ TA:Tb1%; (e) Asn:BOE:Tb1%; (f) (dark field) Asn:BOE:Tb1%; (g) Asn: γ TA:Tb1%.

final composite presented low concentration of Asn as corroborated by the low organic content detected by FTIR.

Photoluminescence

The two hydrated aluminates under consideration have quite different crystal structures, in particular when one considers the way that bigger cations as Ln^{3+} could be accommodated on the Al^{3+} sites. γ - Al_2O_3 has a defect-spinel

structure with most of Al atoms in octahedral coordination and the minority ones in tetrahedral coordination.³ At crystal surface, more distorted tetrahedral Al sites may occur with penta- and hepta-coordinated Al.³¹ γ -Alumina has a lot of structural defects or empty cationic sites, especially near the surface of nano-crystals in poorly crystallized sample, and it has been admitted that Eu^{3+} ions may be accommodated in γ - Al_2O_3 , most probably at these defect sites.^{25,26,32} The crystal structure of boehmite,³³ is orthorhombic. The unit cell consists of two double layers of aluminium-centered distorted octahedral $\text{AlO}_4(\text{OH})_2$. OH groups locate at the outer surface of the double layers and interact to hold the layers together. There is no substitution of Eu^{3+} on the Al^{3+} octahedral sites in boehmite for Eu^{3+} ,²⁴ but that partly hydrated Eu^{3+} ions are directly bonded to OH groups at the boehmite surface. It is highly probable that Tb^{3+} behave the same way as Eu^{3+} , hereafter we discuss characteristic features from the terbium luminescence data that support these hypotheses.

The photoluminescence emission spectra of samples BOE:Tb1% and γ TA:Tb1% are displayed in Figures 4a and 4b, respectively. Characteristic emission bands assigned to the $^5\text{D}_4 \rightarrow ^7\text{F}_j$ transitions ($J = 6, 5, 4, 3$) with the dominant green band at 540 nm are observed. The shape of Tb^{3+} emission is generally little sensitive to the local environment and no additional information could be extracted from their comparison in the two hydrated aluminates. Considering photoluminescence excitation a number of narrow lines assigned to Tb^{3+} ($4f^8$ configuration) $^7\text{F}_6 \rightarrow ^{2S+1}\text{L}_j$ transitions could be observed.³⁴ Of particular interest is the broad contribution observed at wavelengths 320-400 nm since it matches the excitation wavelengths most often encountered in laboratory fluorescence microscopes and supports the consideration of Tb^{3+} as fluorescent bio-label. In addition, an intense broad band at around 240 nm was observed for γ TA:Tb1%, but not for BOE:Tb1%. The strength to the way terbium ions are connected with the host may be responsible for the differences. Two assignments are conceivable for the band around 240 nm. The first assignment is the of Tb^{3+} interconfigurational parity-allowed absorption. From the ground state $^7\text{F}_6$ ($4f^8$), transitions occur to the multiplets $^9\text{D}_j$ and $^7\text{D}_j$ ($4f^7 5d^1$). The former transition (ending at $^9\text{D}_j$) is spin forbidden and occurs at lower energy than the spin allowed one ending at $^7\text{D}_j$.

Dorenbos³⁵ initiated a shift model in the analysis of 5d levels of Tb^{3+} . The spin-allowed transition energies for Tb^{3+} in some mixed oxides (borates or silicates) are actually reported at around 5.20 eV (238 nm). Consistently, Zawadski *et al.*³⁶ assigned the absorption band at 240 nm observed in mixed oxides Al_2O_3 - ZrO_2 : Tb^{3+} to $(4f^8) \rightarrow ^7\text{D}_j$ ($4f^7 5d^1$). All these values agree with the band at 240 nm

(5.17 eV) observed in γ TA:Tb1%. Considering BOE:Tb1%, (Figure 4a) no strong absorption band could be observed, but rather the low energy tail of a stronger excitation truncated by inner filter effect. This would mean that the spin allowed band is shifted towards higher energies, as it is in the aquo ion $[\text{Tb}(\text{OH})_2]_8$ where absorption maximum is at 5.71 eV (217 nm)³⁷ supporting the existence of hydrated terbium ions in boehmite.

The second possible assignment is the host sensitization, which may be described according to the Förster-Dexter energy transfer. A spectral overlap of the host emission with the acceptor absorption is necessary. The visible blue photoluminescence of γ -Al₂O₃ nanoparticles has been investigated in detail by Yu *et al.*³⁸ An emission band peaking at 405 nm, associated with excitations at 236, 245, 255 nm has been observed for γ -Al₂O₃ calcined at 500 °C, and assigned to electron-hole recombination at oxygen defects in the transition alumina. Indeed, the emission background observed for our samples may be assigned to that of the aluminate matrices. The broad emission from alumina overlaps the wavelengths of Tb³⁺ intra 4f⁸ absorption lines (⁷F₆ → ⁵G₆, ⁵D₃, ⁵L₁₀, ⁵L₈, ⁵D₂, ⁵L₈, ⁵H₇), so that γ -Al₂O₃ to acceptor Tb³⁺ energy transfer would occur favorably. Inversely, although a similar photoluminescence occurs for boehmite,^{39,40} there would be no boehmite to terbium energy transfer in BOE:Tb. This can be understood if the bonding of Tb³⁺ with the boehmite is weaker than it is with the transition alumina. So finally both mechanisms would easily explain our observations. An argument in favor of the second assignment that of host sensitization, is given by the consideration of Eu³⁺ in same hosts. The photoluminescence spectra from our preceding work²⁴ are also shown in Figures 4c and 4d. At wavelengths below 300 nm, a broad absorption band was detected for γ TA:Eu1% but not for BOE:Eu1%. This band was assigned to absorption in the localized LMCT state (ligand to metal charge transfer),²⁴ but it could also be due to non radiative energy transfer between the host and Eu³⁺, since the visible emission of aluminates matches the group of absorption lines ⁷F₀ → ⁵D₃, ⁵L₆, ⁵L₇, ⁵D₄.

Also in line with terbium ions having a much more hydrated environment in boehmite than in transition alumina, the ⁵D₄ emission lifetime was shortened due to the enhanced probability of non-radiative de-excitation by the OH vibrators. The ⁵D₄ luminescence decay curves were fitted with first-order exponential functions and the decay time was found to be markedly lower in sample BOE:Tb1% (1.00 ± 0.10 ms) than in sample γ TA:Tb1% (2.56 ± 0.26 ms). Ishizaka *et al.*⁴¹ have measured the ⁵D₄ decay times in Tb³⁺ doped alumina films prepared by sol-gel method, then heat-treated to remove residual water molecules: our observations agree rather well with those

reported on films after heat treatment at 25 °C and at 500 °C, respectively.

Photoluminescence spectra of the nanocomposites Asn:BOE:Tb1% and Asn: γ TA:Tb1% are displayed in Figures 4e and 4f, respectively. Concerning PLE spectra, the main difference between Asn modified or unmodified aluminates were the intensities ratios between the band at 240 nm and ⁷F₆ → ²⁵+¹L_J lines. The broad band appeared clearly in Asn:BOE:Tb1%, whereas it was absent in un-modified boehmite. This observation supports the assumption that host to terbium energy transfer is the cause of this excitation band: indeed, it may be understood that the amine acid strengthens the linkage of hydrated Tb ions with the boehmite surface and favors energy transfer.

Photoluminescence in aqueous medium

After the screening of various amine acid/aluminate/terbium ratios it was established that compositions Tb³⁺/BOE equal 1 or 5 percent and Asn/BOE equal 0.3/1 may be considered as luminescent labels in aqueous media since they remain well dispersed at the nanometric scale in solution. We have thus evaluated the possibility to record the Tb³⁺ luminescence with the measurement conditions usually employed in rare earth luminescent bio-assays: using proper excitation wavelength and optimized time-resolution conditions. Figure 5 shows the emission of Asn:BOE:Tb1% at concentration 0.16 mol L⁻¹ (in mol of Al³⁺) under excitation at 250 or 351nm and with a signal detection fixed from 0.1 milliseconds to 0.5 milliseconds after the exciting pulse.

It is important to establish the lower concentration compatible with the unambiguous observation of time-resolved spectra. In that work, it was checked the luminescence emission up to 0.1 mol L⁻¹ for hybrid in water medium, however the results let us to affirm at the 0.05 mol L⁻¹ as the low limit concentration to time-resolution analysis. The water stability and luminescence behavior could enable the hybrid system to monitor wastewater treatment, e.g., labeling *Escherichia coli*.⁴² Since, *Escherichia coli* and *enterococci* are used as regulatory tools to monitor water and presence of potential enteric pathogens yet their source (human or animal) cannot be determined with routine methods.⁴³

Conclusions

The spray pyrolysis (SP) of aluminium tri-*sec*-butoxide and TbCl₃ in aqueous medium allowed synthesizing nano-structured powders having the crystalline phase of boehmite (noted BOE) or transition alumina γ -Al₂O₃

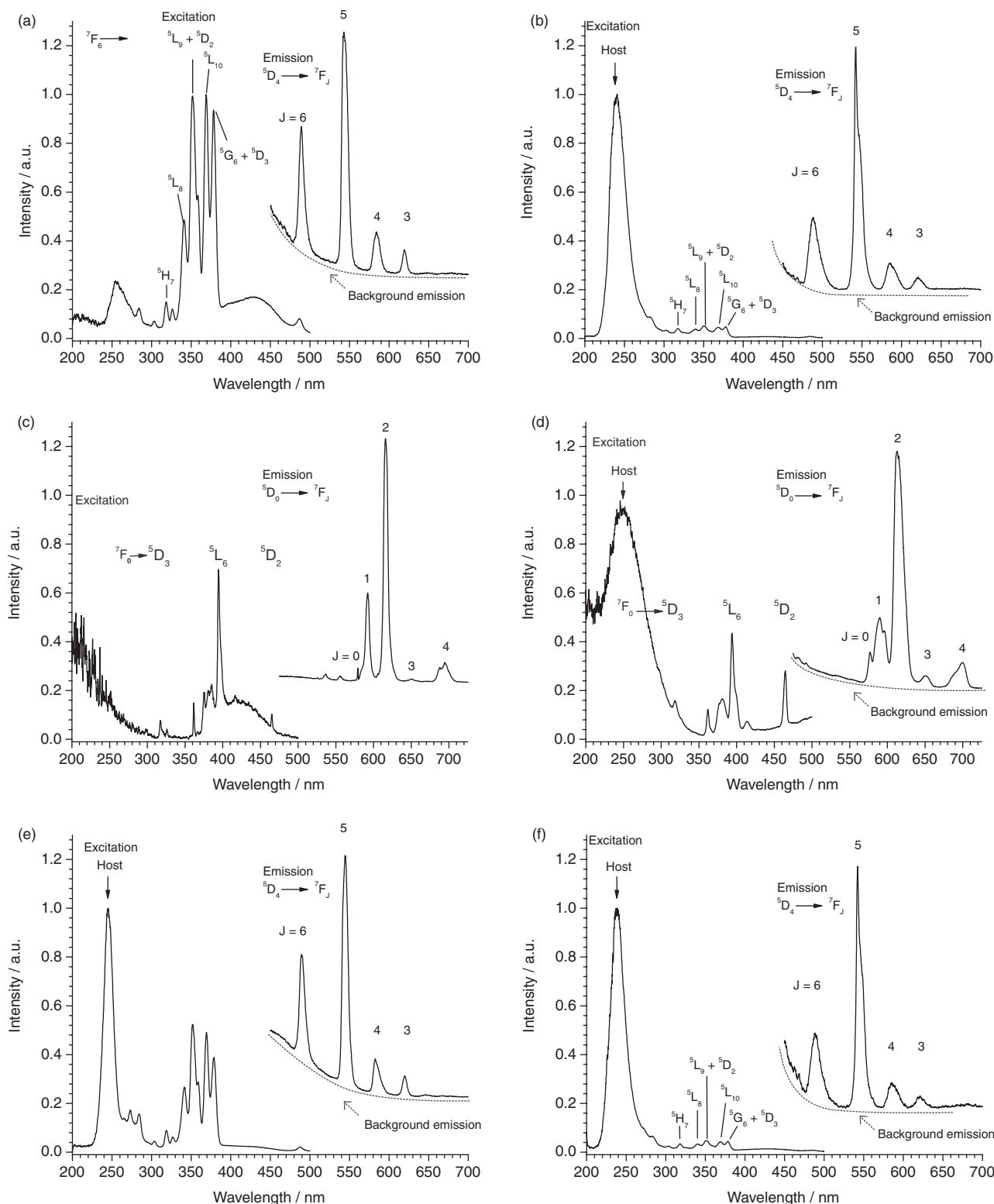


Figure 4. Photoluminescence of (a) BOE:Tb1%; (b) γ TA:Tb1%; (c) BOE:Eu2%; (d) γ TA:Eu2%; (e) Asn:BOE:Tb1%; (f) Asn: γ TA:Tb1%. Excitation spectra monitored at λ emission = 543 nm (a, b, e, f) or at λ emission = 592 nm (c, d); emission spectra by excitation at 351 nm (a), 250 nm (host at b, e, f) and 394 nm (c, d).

(noted γ TA). Particles were spherical and sub-micrometric, consisting of aggregated nanometric sub-particles. The photoluminescence emission spectra of samples

BOE:Tb1% and γ TA:Tb1% exhibited the well-known green emission $^5D_4 \rightarrow ^7F_{J=6-3}$ of Tb^{3+} . The strong near-UV absorption (around 240 nm) is assigned to the host to ion

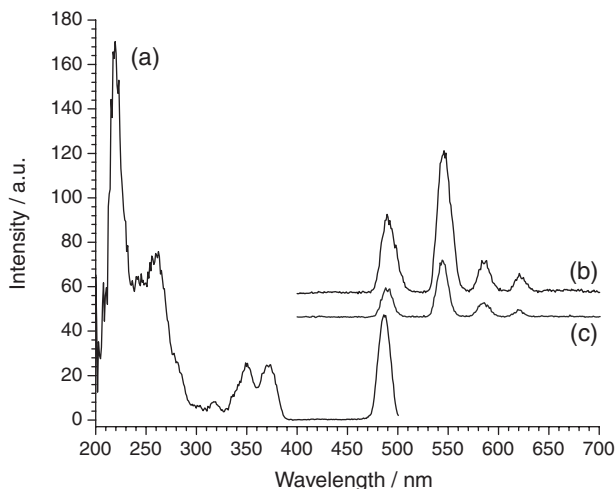


Figure 5. Time resolved photoluminescence of 0.3Asn:BOE:Tb1% 0.16 mol L⁻¹ in water (a) excitation spectra monitored at λ emission = 543 nm and emission spectra by excitation at (b) 250 nm; (c) 351 nm. Delay time at 0.1 ms, sample window as 0.4 ms.

energy transfer. We associate its presence in γ TA:Tb1% to the incorporation of Tb³⁺ in the defect-spinel structure of the γ -Al₂O₃ matrix. In BOE:Tb1%, in contrast, the energy transfer was very weak, confirming our earlier hypothesis that Ln³⁺ ions do not enter the aluminate network in boehmite, but are bonded to the hydroxyls groups at boehmite surface.

The surface of luminescent terbium doped boehmite particles was modified by asparagine Asn. The particles, in (water + Asn), disaggregated into nanoparticles (hydrodynamic diameter from 5 to 100 nm). Asn is localized at the surface of the particles and at the same time the linkage of hydrated terbium ions with boehmite was strengthened, enhancing the aluminate → Tb energy transfer. The goal to get modified aluminate nanoparticles with enhanced luminescence starting from the γ TA:Tb1% was not achieved since it was not possible to disaggregate the sub-micronic spheres in (water + Asn). Besides, γ -Al₂O₃ hydrolysed partially into γ -AlOOH during the reaction with Asn. When homogeneous suspensions in aqueous solution of nanoparticles were achieved, the limit of detection in time-resolution conditions analysis was estimated to 0.05 mol L⁻¹ AlOOH:Tb1%. Spray pyrolysis is a cheap, fast and reliable production process. It is well adapted to the synthesis of hydrated aluminate particles. Moreover aluminates particles may be doped with any luminescent lanthanide Ln leading to strong photoluminescence in the visible, with a millisecond lifetime appropriated for efficient time gated detection. With a highly reactive surface, terbium-doped boehmite nanoparticles may be easily modified and therefore fulfill several of the key features for their actual use for *in vitro* or *in vivo* applications.

Acknowledgements

Authors thank Y. Kihn (CEMES-CNRS) and C. Galaup (SPCMIB-Université de Toulouse) for their support in electron microscopy and time-resolved luminescence investigations, respectively. The Brazilian agencies FAPESP (2007/55723-6, 2011/21551-0), CNPq, CAPES, and the CAPES-COFECUB Brazil-France cooperation program for the grant to J. M. A. C. are also acknowledged.

References

1. Penilla, E. H.; Kodera, Y.; Garay, J. E.; *Adv. Funct. Mater.* **2013**, *23*, 6036.
2. Zhou, R. S.; Snyder, R. L.; *Acta Crystallogr.* **1991**, *B47*, 617.
3. Sohlberg, K.; Pennycook, S. J.; Pantelides, S. T.; *J. Am. Chem. Soc.* **1999**, *121*, 7493.
4. Pecharrmán, C.; Sobrados, I.; Iglesias, J. E.; González-Carreño, T.; Sanz, J.; *J. Phys. Chem. B* **1999**, *103*, 6160.
5. Krokidis, X.; Raybaud, P.; Gobichon, A.-E.; Rebours, B.; Euzen, P.; Toulhoat, H.; *J. Phys. Chem. B* **2001**, *105*, 5121.
6. Paglia, G.; Rohl, A. L.; Buckley, C. E.; Gale, J. D.; *Phys. Rev. B* **2005**, *71*, 224115.
7. Alvarez, L. J.; Leon, L. E.; Sanz, J. F.; Capitan, M. J.; Odriozola, J. A.; *J. Phys. Chem.* **1995**, *99*, 17872.
8. Yoldas, B. E.; *J. Mater. Sci.* **1975**, *10*, 1856.
9. Yoldas, B. E.; *Ceramic Bulletin* **1975**, *54*, 289.
10. Granados-Correa, F.; Jiménez-Becerril, J.; *J. Hazard. Mater.* **2009**, *162*, 1178.
11. Yoon, T. H.; Johnson, S. B.; Musgrave, C. B.; Brown Jr., G. E.; *Geochim. Cosmochim. Acta* **2004**, *68*, 4505.
12. Landry, C. C.; Pappé, N.; Mason, M. R.; Apblett, A. W.; Tyler, A. N.; MacInnes, A. N.; Barron, A. R.; *J. Mater. Chem.* **1995**, *5*, 331.
13. Kareiva, A.; Harlan, C. J.; MacQueen, D. B.; Cook, R. L.; Barron, A. R.; *Chem. Mater.* **1996**, *8*, 2331.
14. Kang, H.-J.; Kim, D. J.; Park, S.-J.; Yoo, J.-B.; Ryu, Y. S.; *Thin Solid Films* **2007**, *515*, 5184.
15. Kapoor, S.; Hegde, R.; Bhattacharyya, A. J.; *J. Control. Release* **2009**, *140*, 34.
16. Al-Kattan, A.; Santran, V.; Dufour, P.; Dexpert-Ghys, J.; Drouet, C.; *J. Biomater. Appl.* **2014**, *28*, 697.
17. Li, L.; Liu, Y.; Tao, J.; Zhang, M.; Pan, H.; Xu, X.; Tang, R.; *J. Phys. Chem. C* **2008**, *112*, 12219.
18. Meiser, F.; Cortez, C.; Caruso, F.; *Angew. Chem. Int. Ed.* **2004**, *43*, 5954.
19. Jin, D.; Connally, R.; Piper, J.; *Cytom. Part A* **2007**, *71A*, 783.
20. Okada, K.; Tanaka, A.; Hayashi, S.; Otsuka, N.; *J. Mater. Sci. Lett.* **1993**, *12*, 854.

21. Vallet-Regi, M.; Rodriguez-Lorenzo, L. M.; Ragel, C. V.; Salinas, A. J.; Gonzalez-Calbet, J. M.; *Solid State Ionics* **1997**, 101-103, 197.
22. Kato, T.; *J. Ceram. Soc. Jpn.* **2002**, 110, 146.
23. Caiut, J. M. A.; Dexpert-Ghys, J.; Kihn, Y.; Vérelst, M.; Dexpert, H.; Ribeiro, S. J. L.; Messaddeq, Y.; *Powder Technol.* **2009**, 190, 95.
24. Caiut, J. M. A.; Ribeiro, S. J. L.; Messaddeq, Y.; Dexpert-Ghys, J.; Verelst, M.; Dexpert, H.; *Nanotechnology* **2007**, 18, 455605.
25. Marques, R. F. C.; Caiut, J. M. A.; Paiva-Santos, C. O.; Ribeiro, S. J. L.; Messaddeq, Y.; Garcia, C.; Neumeyer, D.; Dexpert, H.; Verelst, M.; Dexpert-Ghys, J.; *Braz. J. Phys.* **2009**, 39, 176.
26. Caiut, J. M. A.; Bazin, L.; Mauricot, R.; Dexpert, H.; Ribeiro, S. J. L.; Dexpert-Ghys, J.; *J. Non-Cryst. Solids* **2008**, 354, 4860.
27. Fripiat, J. J.; Bosmans, H.; Rouxhet, P. G.; *J. Phys. Chem.* **1967**, 71, 1097.
28. Boumaza, A.; Favaro, L.; Lédion, J.; Sattonnay, G.; Brubach, J. B.; Berthet, P.; Huntz, A. M.; Roy, P.; Tétot, R.; *J. Solid State Chem.* **2009**, 182, 1171.
29. Wang, S.-L.; Johnston, C. T.; Bish, D. L.; White, J. L.; Hem, S. L.; *J. Colloid Interface Sci.* **2003**, 260, 26.
30. Cooper, S. J.; *Langmuir* **2002**, 18, 3749.
31. Alvarez, L. J.; Leon, L. E.; Sanz, J. F.; Capitan, M. J.; Odriozola, J. A.; *J. Phys. Chem.* **1995**, 99, 17872.
32. Monteiro, M. A. F.; Brito, H. F.; Felinto, M.; Brito, G. E. S.; Teotonio, E. E. S.; Vichi, F. M.; Stefani, R.; *Micropor. Mesopor. Mat.* **2008**, 108, 237.
33. Milligan, W. O.; McAtee, J. L.; *J. Phys. Chem.* **1956**, 60, 273.
34. Carnall, W. T.; Crosswhite, H.; Crosswhite, H. M.; *Energy Level Structure and Transition Probabilities in the Spectra of the Trivalent Lanthanides in LaF₃*, 1st ed.; Argonne National Laboratory: Argonne, USA, 1977.
35. Dorenbos, P.; *J. Phys. Condens. Matter* **2003**, 15, 6249.
36. Zawadski, M.; Hreniak, D.; Wrzyszc, J.; Mista, W.; Grabowska, H.; Malta, O. M.; Strek, W.; *Chem. Phys.* **2003**, 291, 275.
37. Carnall, W. T.; *J. Chem. Phys.* **1968**, 49, 4412.
38. Yu, Z. Q.; Li, C.; Zhang, N.; *J. Lumin.* **2002**, 99, 29.
39. Yu, Z. Q.; Wang, C. X.; Gu, X. T.; Li, C.; *J. Lumin.* **2004**, 106, 153.
40. Bai, X.; Caputo, G.; Hao, Z.; Freitas, V. T.; Zhang, J.; Longo, R. L.; Malta, O. L.; Ferreira, R. A. S.; Pinna, N.; *Nat. Commun.* **2014**, 5, 5702.
41. Ishizaka, T.; Nozaki, R.; Kurokawa, Y.; *J. Phys. Chem. Solids* **2002**, 63, 613.
42. Duarte, A. P.; Mauline, L.; Gressier, M.; Dexpert-Ghys, J.; Roques, C.; Caiut, J. M. A.; Deffune, E.; Maia, D. C. G.; Carlos, I. Z.; Ferreira, A. A. P.; Ribeiro, S. J. L.; Menu, M.-J.; *Langmuir* **2013**, 29, 5878.
43. Srinivasan, S.; Aslan, A.; Xagorarakis, I.; Alocilja, E.; Rose, J. B.; *Water Res.* **2001**, 45, 2561.

Submitted: June 17, 2015

Published online: August 25, 2015

FAPESP has sponsored the publication of this article.